# Al stabilized TiC twinning platelets

Hui Zhang
*High-Performance Ceramic Division, Shenyang National Laboratory for Materials Science, Institute of Metal Research, Chinese Academy of Sciences, Shenyang 110016, China; and University of Chinese Academy of Sciences, Beijing 100049, China*

Xiaohui Wang
*High-Performance Ceramic Division, Shenyang National Laboratory for Materials Science, Institute of Metal Research, Chinese Academy of Sciences, Shenyang 110016, China*

Zhaojin Li
*High-Performance Ceramic Division, Shenyang National Laboratory for Materials Science, Institute of Metal Research, Chinese Academy of Sciences, Shenyang 110016, China; and University of Chinese Academy of Sciences, Beijing 100049, China*

Yanchun Zhou[a)]
*Science and Technology of Advanced Functional Composite Laboratory, ARIMPT, Beijing 100076, China*

(Received 11 February 2014; accepted 25 March 2014)

Titanium carbide (TiC) twins are believed to be extremely unstable because of their high twin boundary energy. Here, we report that TiC twins are always presented in platelets with dimensions of 2–3 μm in length and less than 300 nm in width. In-depth microstructural characterizations by high-resolution transmission electron microscopy demonstrate that Al atoms at the twin boundary play a decisive role in stabilizing TiC twins. With different amounts of Al, perfect and defective TiC twins are formed. For perfect twins, three types of twin boundaries can be formed depending on the amount of remaining Al at the twin boundary. With inadequate Al, the TiC twins become defective with certain degrees of deviation from the perfect twin orientation. Based on a detailed analysis of the microstructure of the twin boundaries, a mechanism for the formation and stabilization of TiC twins is proposed.

## I. INTRODUCTION

Titanium carbide (TiC) is of technological importance and has vast industrial applications because of its low density, high hardness, and high strength. To improve the mechanical performance of TiC and TiC-containing composites, the grain size and morphology of TiC have been tailored to modulate the mechanical properties.[1–5] As a new way to improve the mechanical properties of metals and ceramics,[6–8] nanotwins have been introduced into TiC (as well as other carbides) containing composites.[9–13]

The stacking-fault energy (SFE) of TiC is in the range between 130 and 300 mJ/m$^2$.[14,15] Therefore, TiC twins are extremely unstable from an energetic point of view, and there have been few reports of deformation or growth twins in bulk TiC samples. Nonetheless, research on the stacking faults (SFs) and microtwins of TiC has been reported in the literature. Venables et al.[16] found that the SFs of TiC are associated with impurity atoms. Kooi et al.[14] proposed that Si can induce SFs in TiC grains. Yu et al.[11] further confirmed that Al atoms can reduce the SFE of TiC. Through the de-intercalation of Al atoms in $Ti_3AlC_2$, Zhang et al.[17] synthesized $TiC_x$–Cu composites with TiC nanotwins. However, to the best of our knowledge, the successful synthesis of TiC twins with large size has not been reported. This is partially due to the lack of knowledge of the microstructure and stabilization mechanism of TiC twins.

It is noted that the reports on the TiC twins are mainly limited to the layered ternary ceramics following a general formula $Ti_nA_mC_{n-m}$ (A is Al and/or Si and $n \geq 2m$), and corresponding composites due to the unique crystal structure of $Ti_nA_mC_{n-m}$. For example, the crystal structure of $Ti_3AlC_2$ can be considered as the alternative stacking of $Ti_3C_2$ and Al atomic layers, as shown in Fig. 1(a). With minute distortions of the $Ti_6C$ octahedra, the $Ti_3C_2$ layers are extremely similar to the counterparts in TiC twins,[18,19] as shown in Fig. 1(b). The adjacent $Ti_3C_2$ layers are in twin orientation. Therefore, different from the deformation and growth twins, microtwinned $Ti_3C_2$ can be formed directly by the de-intercalation of the Al layer. However, the microtwinned $Ti_3C_2$ is unstable due to the high twin boundary energy (TBE). The microtwinned $Ti_3C_2$ will completely de-twin and become normal $TiC_x$, if certain stabilizing mechanism is not available.

a)Address all correspondence to this author.
e-mail: yczhou714@gmail.com
DOI: 10.1557/jmr.2014.80

 © Materials Research Society 2014 

https://doi.org/10.1557/jmr.2014.80 Published online by Cambridge University Press

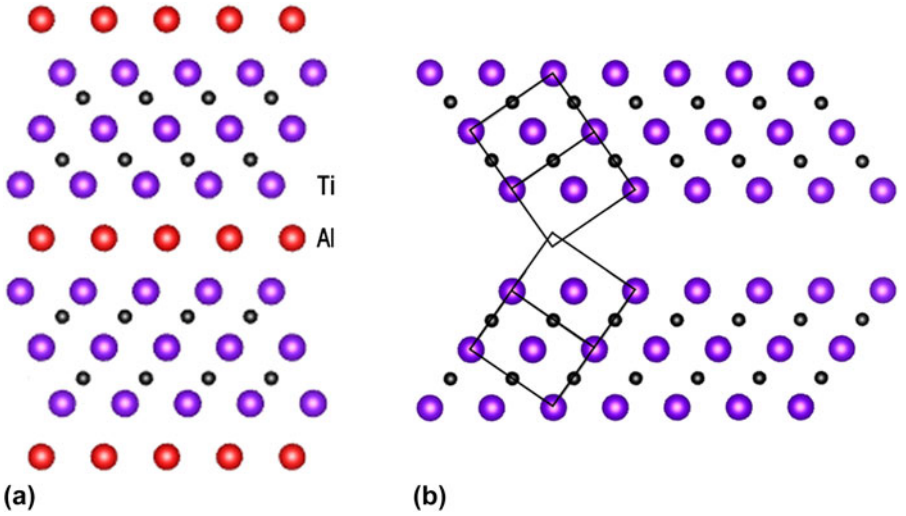



FIG. 1. (a) Projection of $Ti_3AlC_2$ along the $[11\bar{2}0]$ axis. (b) Projection of the corresponding part of the $Ti_3C_2$ layer in TiC twins along the $[1\bar{1}0]$ axis. The dark lines demonstrate the unit cell of TiC. The Ti, Al, and C atoms are presented in violet, red, and black, respectively.

Theoretically, it has been proposed that the Al atoms can stabilize the TiC twins. Yu et al. constructed a coherent twin boundary (CTB) model and calculated the TBE.[11] They proposed that Al (and/or Si) can lower the TBE with the formation of π bonding between carbon neighbors of Si/Al atoms. However, Zhang et al.[17] pointed out that the TiC twin boundary is not coherent and no Al elements were detected in the twins. Moreover, they constructed a TiC twin model with two layers of Ti atoms in direct contact, where the incoherent twin boundary (ITB) was not ideally mirror-symmetric. Thus, two basic but important questions remain unanswered unambiguously: (1) What exactly is the stabilization mechanism of the TiC twins? (2) Is the twin boundary a CTB or ITB?

In the present work, TiC twinning platelets were synthesized by the reaction of $Ti_3AlC_2$ and Ni. In addition, the microstructures were studied in detail by high resolution transmission electron microscopy (HRTEM) to elucidate the formation and stabilization mechanism of TiC twinning platelets with large size.

## II. EXPERIMENTAL DETAILS

TiC twinning platelets were synthesized by the in situ reaction between $Ti_3AlC_2$ (−300 mesh) and Ni (−300 mesh; Sinopharm Chemical Reagent Co., Ltd., Shanghai, China) powders. The $Ti_3AlC_2$ powders were synthesized using the previously reported solid–liquid reaction method.[20] The TiC twin-containing composite was prepared by the following procedure. First, the $Ti_3AlC_2$ and Ni powders with a molar ratio of 1:2 were mixed with absolute ethanol and agate balls in an agate jar for 12 h, followed by drying at 60 °C for 10 h. The homogenized powders were then uniaxially pressed into a green compact in a graphite mold with an inner diameter of 50 mm. Subsequently, the green compact, together with the mold, was put into a hot pressing furnace and heated to 1350 °C at a heating rate of 10 °C/min under Ar flow and held for 1 h at a pressure of 30 MPa. Finally, the sample was allowed to cool naturally to room temperature in the furnace.

For transmission electron microscopy investigation, a 4 mm × 4 mm slice was cut from the bulk sample and ground to a thickness of approximately 30 μm. The slice was then dimpled with a Gatan 656 Dimple Grinder and made electron transparent by Ar-ion-milling using a Gatan 691 Precision Ion Polishing System. X-ray diffraction (XRD) patterns were collected using an x-ray diffractometer (Rigaku D/max-2400, Tokyo, Japan) with Cu $K_\alpha$ radiation. Microstructural characterization was performed using a transmission electron microscope (FEI Tecnai G2 F20, Hillsboro, OR) working at 200 kV with an energy dispersive spectroscopy detector and a high-angle annular dark-field detector in the scanning transmission electron microscopy (STEM) system.

## III. RESULTS

### A. TiC twinning platelets

Figure 2(a) is a typical transmission electron microscopy (TEM) bright field image of the formed platelets (labeled with pink asterisks). The electron diffraction pattern (EDP) is shown in Fig. 2(b), where the diffraction spots belonging to different grains are linked by lines of different colors, indicating that the platelets are TiC twins. The TiC platelets have dimensions of 2–3 μm in length and less than 300 nm in width, with an aspect ratio (length-to-width) of about 10. SFs were observed in the TiC

https://doi.org/10.1557/jmr.2014.80 Published online by Cambridge University Press

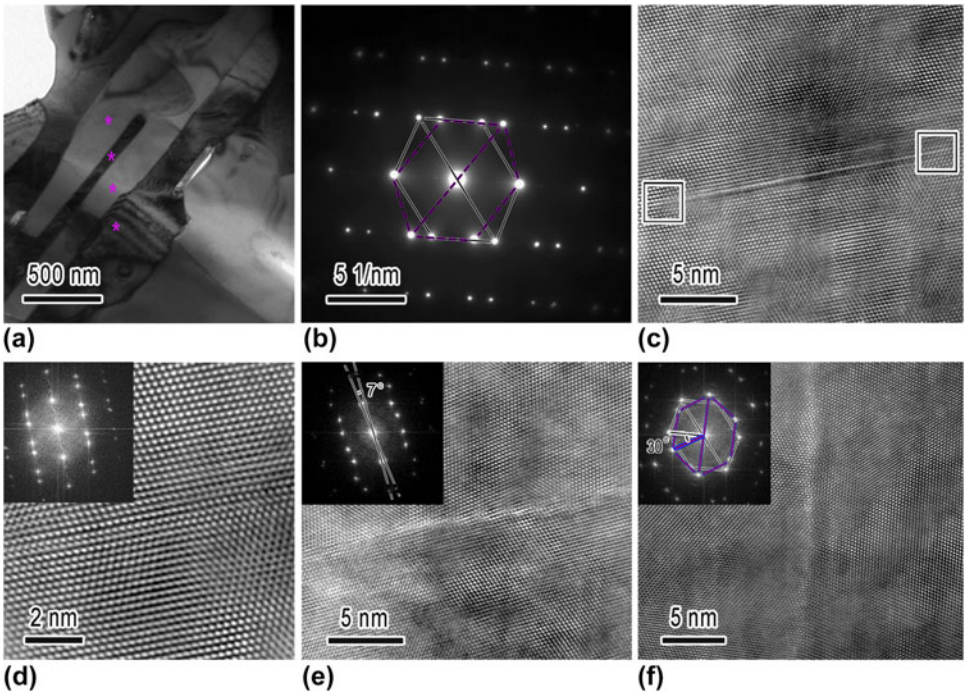



FIG. 2. (a) Typical TEM bright field image of TiC twinning platelets, adapted from Ref. 13. (b) Representative EDP of TiC twins. The diffraction spots belonging to different grains are linked by lines in different colors. (c) HRTEM image of a stacking fault inside the twin. The squares mark the irradiated regions by electron beam. (d–f) HRTEM image of perfect TiC twins (d), defective twins with 7° (e), and 30° (f) deviations from the perfect twin orientation.

twinning platelets. As shown in Fig. 2(c), the SF involves one or two {111} planes. The SF is extremely sensitive to the electron beam. For example, it disappeared immediately when the square region was exposed to the electron beam during the experiment. Interestingly, some regions of the twinning platelets are not perfectly twinned. For comparison, the HRTEM images of perfect and defective twins are presented in Figs. 2(d)–2(f), where the insets are the corresponding fast Fourier transform patterns. In contrast to the perfect twins shown in Fig. 2(d), there is a certain degree of deviation from the perfect twin orientation in the defective twins, for example, 7° in Fig. 2(e) and 30° in Fig. 2(f).

## B. Twin boundary of TiC

To further understand the TiC twins, the microstructure of the twin boundary was studied by means of HRTEM. In contrast to the results of Zhang et al.[17] and Yu et al.,[10] three types of twin boundaries were observed in the present work. The HRTEM images of the twin boundaries are shown in Fig. 3. The twin boundary in Fig. 3(a) is CTB type. The measured angles between $(\bar{1}\,\bar{1}1)$ and (111) are 71° and 70°, consistent with the calculated angle of 70.5°. The two parts on either side of the twin boundary are ideally mirror-symmetric with respect to the twin boundary, with a Ti atomic layer as the mirror plane, which is consistent with the first-principles calculations.[11] Unlike CTB, the two parts on either side of the twin boundary in Fig. 3(b) are not ideally mirror-symmetric with respect to the twin boundary, although the measured angles between $(\bar{1}\,\bar{1}1)$ and (111) (73° and 70°) are also consistent with the calculated value (70.5°). Translation along the (111) plane occurs, forming ITB with one Ti atomic plane as the twin boundary. It is worth noting that the atoms at the twin boundary belong to neither of the two twinned parts. Another type of ITB is shown in Fig. 3(c). Similar to the ITB in Fig. 3(b) but dissimilar to the CTB, translation along the (111) plane occurs, which is ascribed to the electrostatic repulsion between the adjacent Ti atoms, as described by Zhang and co-workers.[17] The ITB consists of two Ti atomic layers. To distinguish the two types of ITBs, the ITB in Figs. 3(b) and 3(c) is represented as ITB1 and ITB2, respectively. Interestingly, the coexistence of CTB and ITB was observed, as shown in Fig. 3(d).

## C. Transient $TiC_x$

It is worth noting that complex EDP, as shown in Fig. 4(a), can be observed occasionally in the TiC twinning platelets. The circled weak diffraction spots perform a 3-fold modulation on the basic diffraction spots generated by TiC twins. The extra diffraction spots are generated by transient $TiC_x$. The HRTEM image is presented in Fig. 4(b); the inset is a rotated and filtered HRTEM image of the transient $TiC_x$. The 3-fold modulation on the (111) plane of TiC can be clearly seen. The modulations on the (111) plane of TiC are similar to those reported by Zhou et al.[19]

https://doi.org/10.1557/jmr.2014.80 Published online by Cambridge University Press

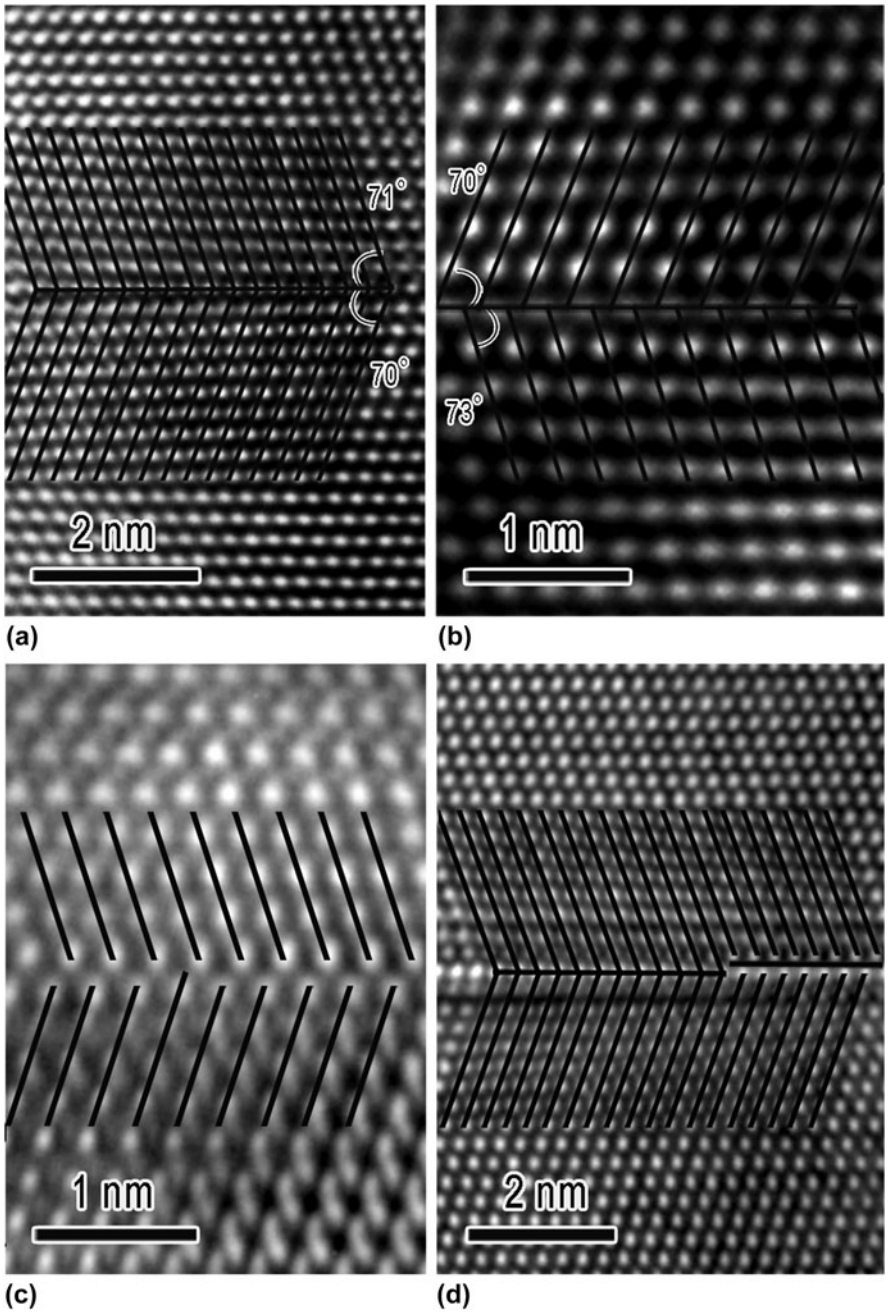



FIG. 3. HRTEM image of twins with (a) CTB, (b) ITB1, (c) ITB2, and (d) both CTB and ITB2.

and Zhang et al.[17] The lattice parameter $c$ calculated according to the weak diffraction spots and the HRTEM image in the inset of Fig. 4(b) is 7.43 Å, if the weak diffraction spot nearest to the transmission spot is indexed as (0001). This value is close to half that of h-$TiC_x$ (14.60 Å)[17] and larger than half that of $Ti_2AlC$ (13.60 Å). Thus, the complex EDP cannot be produced by the well-aligned TiC and $Ti_2AlC$.[21] If the weak diffraction spots were generated by h-$TiC_x$ ($P3m1$), all the (000$l$) diffraction spots should be visible. However, this is not consistent with the periodicity calculated from the EDP, where $c$ is 7.43 Å, only half that of h-$TiC_x$. Therefore, it is believed that a new structure shown in Fig. 4(c), $Ti_3C_2$, which is only half of the unit cell of h-$TiC_x$, generated the weak diffraction spots. Using the crystal structure of $Ti_3C_2$, HRTEM was simulated with the "HRTEM" module of the Cerius[2] computational program for material research (Molecular Simulation Inc., San Diego, CA, USA). The montage of the best-matched experimental and simulated images is presented in Fig. 4(d). It is clear that the simulated and experimental HRTEM images are remarkably similar.

https://doi.org/10.1557/jmr.2014.80 Published online by Cambridge University Press

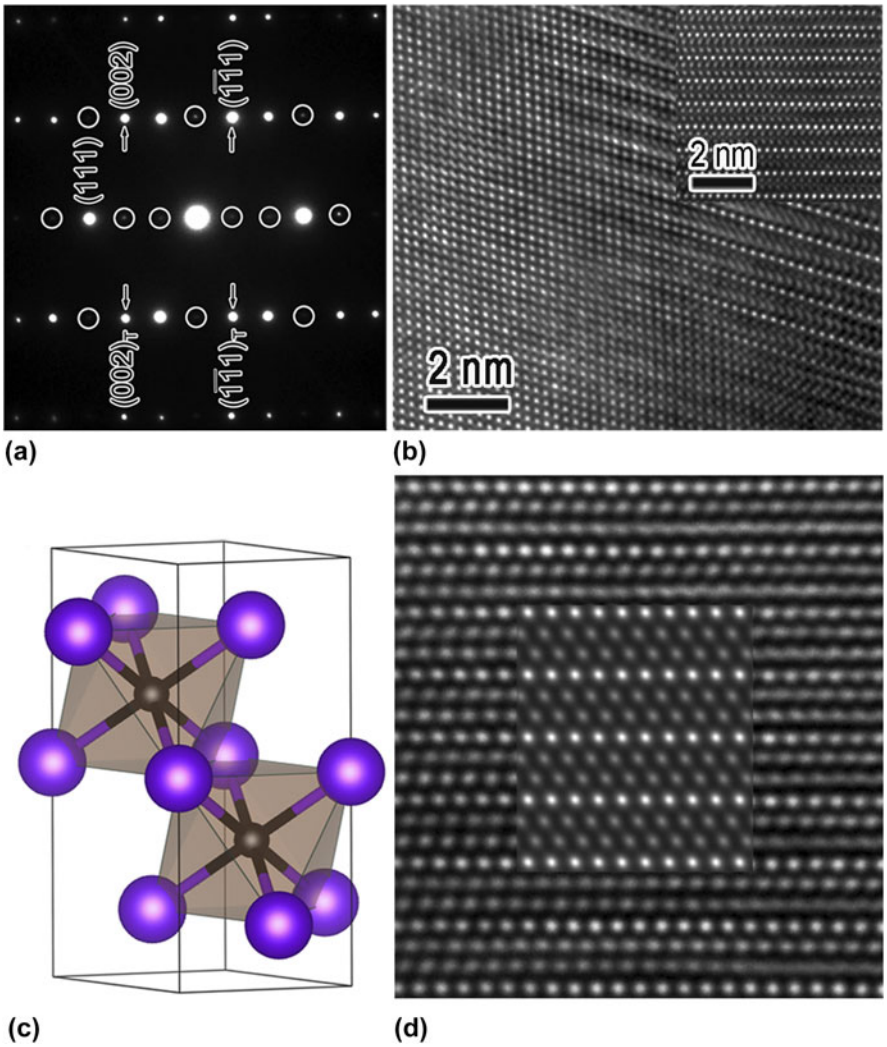



FIG. 4. (a) Complex EDP of TiC twins. (b) HRTEM image of the interface. Inset is a rotated and filtered HRTEM image of $Ti_3C_2$. (c) Unit cell of $Ti_3C_2$. The Ti and C atoms are presented in violet and black, respectively. (d) Montage of the experimental and simulated HRTEM images of $Ti_3C_2$.

### D. Chemical composition of the TiC twins

The TBE of TiC is quite high, thus TiC twins are commonly recognized to be extremely unstable.[14] Yu et al. proposed that Al atoms can reduce the TBE of TiC and detected Al in TiC grains with high-density SFs by means of energy dispersive x-ray microanalysis (EDX).[11] On the other hand, Zhang et al. proposed that no impurities (Al) remained at the twin boundaries.[17] To elucidate the stabilization mechanism of TiC twinning platelets in the present study, the chemical composition of TiC twins was studied in detail using EDX in TEM and STEM mode and the results are presented in Fig. 5. To enhance the intensity of the signals generated by the impurities, TiC twinning platelets with much smaller width were chosen for analysis, as shown in the inset of Fig. 5(a). The EDX spectrum is demonstrated in Fig. 5(a). It is clear that there are some amounts of Al (approximately 1%) in the TiC twinning platelets. (In contrast, there is no detectable Al in the TiC matrix.) To determine the distribution of Al in the platelets, STEM-EDX mapping was conducted in the drift-corrected spectrum image scanning mode. The results are displayed in Fig. 5(b), which is a montage of the morphology and EDX map of Al–K. It can be seen that Al is segregated at the twin boundaries. It is worth noting that the distribution of Al in the twin boundaries is not homogeneous (i.e., some twin boundaries contain more Al than others).

## IV. DISCUSSION

### A. Structure of the twin boundary

The structure of twin boundaries for the face-centered cubic crystals has been studied by many researchers.[22–25] In general, $\Sigma3\{111\}$ is a CTB and $\Sigma3\{112\}$ is an ITB.

https://doi.org/10.1557/jmr.2014.80 Published online by Cambridge University Press

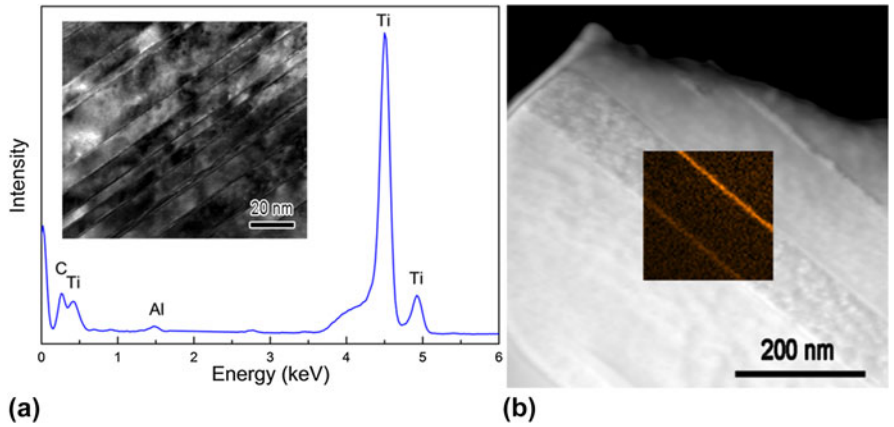



FIG. 5. (a) TEM-EDX spectrum of TiC twinning platelets. Inset shows the TEM bright image of the platelets. (b) Montage of STEM morphology and an EDX map of Al–K.

Yu et al. noted that the Σ3{111} twin boundaries in TiC microtwins are coherent.[10] However, Zhang et al. subsequently reported that the Σ3{111} twin boundaries of TiC twins are incoherent.[17] As shown in Figs. 3(a)–3(c), both the CTB and ITB were observed in the present study. The ITB1 in Fig. 3(b) is closely related to the CTB in Fig. 3(a). The CTB will become the ITB1, if the two parts on either side of the twin boundary translate slightly along the (111) plane. Similarly, ITB1 will become ITB2 [Fig. 3(c)], if the atoms at the twin boundary are merged into one of the twinned parts after translation. The translation-induced transformation from CTB to ITB is supported by the coexistence of CTB and ITB, as shown in Fig. 3(d). Apart from translation along the (111) plane, rotation along the $[1\bar{1}0]$ axis was also observed, as presented in Figs. 2(e) and 2(f). Both the translation and rotation originate from the instability of the twin boundary. In the absence of adequate stabilizing element (i.e., Al), the CTB cannot persist. As a result, translation along the (111) plane occurs, forming the ITB to avoid the configuration of directly and head-to-head contacted Ti atoms in the twin boundary (see the latter section). With less stabilizing element, de-twinning will be initiated, resulting in the rotation along the $[1\bar{1}0]$ axis [Figs. 2(e) and 2(f)]. As demonstrated in Fig. 5(b), the distribution of Al among the twin boundaries is inhomogeneous. Thus, the twin boundaries exist in various types, being perfect or defective and coherent or incoherent.

## B. Formation and stabilization mechanism of TiC twinning platelets

The SFE and TBE are closely related. In general, the TBE is proportional to the SFE. The SFE of TiC is 130–300 mJ/m$^2$, depending on the C/Ti ratio. No SFs have been observed in the stoichiometric TiC, even when it has been subjected to severe deformation.[14] Thus, TiC twins are extremely unstable from an energetic point of view, and consequently, there have been very few reports of TiC twins with large size. Kooi et al.[14] observed TiC microtwins that involved three to five {111} layers at the regions where SFs existed. They ascribed the formation of SFs to the presence of Si. Yu et al.[11] studied the effect of Al on twin stabilization experimentally and theoretically. They found that the TBE of pure TiC is extremely high (927 mJ/m$^2$) and that of Al-doped TiC is −0.073 mJ/m$^2$, and therefore concluded that twins and SFs can form spontaneously in Al-doped TiC. However, no twins but only high density SFs were observed experimentally by Yu et al. Zhang et al.[17] observed TiC twins in a $TiC_x$–Cu composite, but the twins were only a few dozens of nanometers in size. Thus, it is surprising that TiC twinning platelets with large size (2–3 μm in length) can be formed and remain after keeping 1 h at 1350 °C.

To account for the formation and stabilization of TiC twinning platelets, considering the presence of SFs, defective twins and ITBs in the TiC platelets, as well as the inhomogeneous segregation of Al at the twin boundaries (no detectable Al was observed at the normal TiC grain boundaries), a possible mechanism is illustrated in Fig. 6. Briefly, the formation of TiC twins can be divided into four steps. First, Al atoms de-intercalate out of $Ti_3AlC_2$ grains and react with Ni to form $Ni_3Al$ (the XRD pattern is not shown here for brevity), resulting in the formation of a $Ti_3C_2$ microtwinned structure, as shown in Figs. 6(a) and 6(b). It is worth noting that some Al remained at the twin boundaries, as demonstrated in Fig. 5(b). Thus, some Al atoms will remain in the $Ti_3C_2$ microtwinned structure as impurities [Fig. 6(b)]; this will be discussed in detail later. Second, relaxation of the $Ti_3C_2$ microtwinned structure takes place. The Ti atoms in direct contact with each other are extremely unstable and will translate as a result of electrostatic repulsion, as illustrated in Fig. 6(c). The microtwinned structure is similar to the crystal structure shown in Fig. 4(c). With further relaxation and ordering, the microtwinned structure will become $Ti_3C_2$. Because the sample used in the present study was synthesized at

https://doi.org/10.1557/jmr.2014.80 Published online by Cambridge University Press

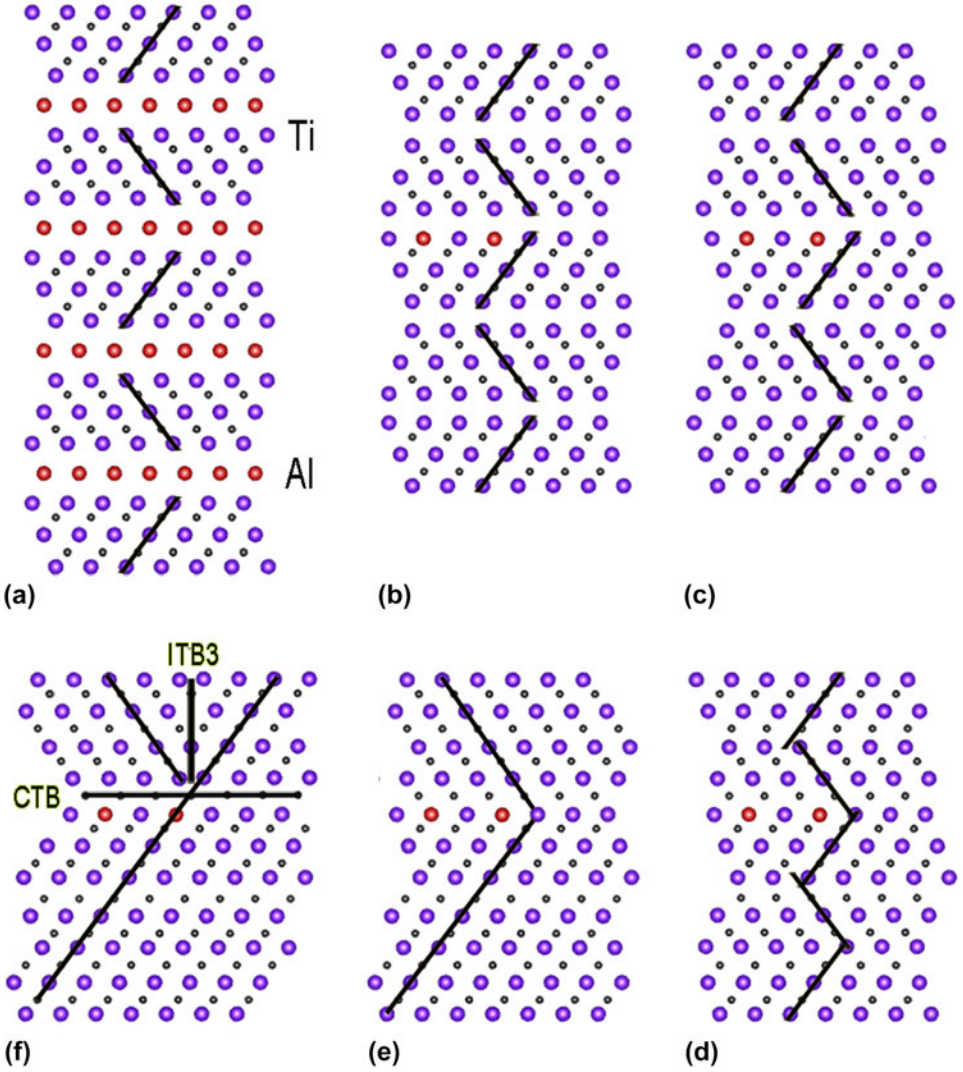



FIG. 6. (a) Projection of $Ti_3AlC_2$ along the [11$\bar{2}$0] axis. The Ti, Al, and C atoms are presented in violet, red, and black, respectively. (b) Al de-intercalated structure with some remaining Al atoms; (c) relaxed structure by the translation of the $Ti_3C_2$ atomic layers; (d) Ti out-diffused structure; (e) TiC twinning layers merge into nanotwins, where the regions without Al atoms merge into one large twinning lamella; and (f) TiC twinning platelets with the coexistence of Σ3{111} and Σ3{112} twin boundaries, similar to that in Fig. 2(a). The dark lines are the counterparts of the (002) plane of TiC. The volume change is not considered in the illustrations for the sake of simplicity.

1350 °C, which was 200 °C higher than the temperature used by Zhang et al.,[17] and theoretically, one third of Ti atoms will react with Ni, well-crystallized $Ti_3C_2$ was only sporadically observed in the present study. Third, de-intercalation of Ti atoms occurs. Although the Ti atomic layers in direct contact have been relaxed by translation, Ti atoms still have high energy and can easily diffuse out of the unstable structure to react with $Ni_3Al$ and Ni to form $Ni_2AlTi$, resulting in asymmetric TiC microtwins, as illustrated in Fig. 6(d). It is worth noting that the third step does not necessarily take place later than the second step. Finally, the resulting asymmetric TiC microtwins without Ti atoms in direct contact are still unstable and the adjacent twinned layers will de-twin and merge to form TiC nanolaminates to reduce the twin boundaries, resulting in TiC twinning platelets of large size, as shown in Figs. 6(e) and 6(f). The twin boundaries with Al impurities still remain and only CTB is sketched in Fig. 6(e). In fact, with different amounts of Al, the twin boundaries can be CTB, ITB1, or ITB2 and can even become defective twins. If the de-twinning and merging processes do not proceed to completion, SFs will be formed at the original twin boundaries, as demonstrated in Fig. 2(c). The whole process can produce unique TiC twin morphologies with Σ3{112} ITB (labeled as ITB3), as illustrated in Fig. 6(f). This is similar to the morphology observed in Fig. 2(a).

Theoretically, the $Ti_3AlC_2$ grains will completely react with Ni to form TiC and $Ni_2AlTi$, the fourth step will completely remove the twinned structure, and no TiC

https://doi.org/10.1557/jmr.2014.80 Published online by Cambridge University Press

twins will remain. In fact, the ternary phase diagram of Ni–Al–Ti shows that $Ni_2AlTi$ can exist over a wide range of compositions.[26,27] Experimentally, the Al content is always determined to be sub-stoichiometric.[27] Thus, it is not difficult to understand that some Al will remain in the TiC, as presented in Fig. 5(a). Similar to the impurities in the other ceramic grain boundaries,[28–32] the remaining Al atoms were observed to segregate at the twin boundaries, as shown in Fig. 5(b). According to the results of Yu et al.,[11] the presence of Al atoms will help stabilize the TiC twins, and thus, the nanotwinned structure will be retained to some extent.

The proposed mechanism can quantitatively explain why the TiC twins are of small size but high density in the experiment conducted by Zhang et al., whereas they are of large size and not of high density in the present study. In the work of Zhang et al., $TiC_x$ was formed by the de-intercalation of Al out of $Ti_3AlC_2$ grains to form solid solutions with Cu. According to the composition analysis of Cu–30 vol% $TiC_x$ composite, the nominal formula of $TiC_x$ is $Ti_3Al_{0.17}C_{2.82}$.[9] The high-density TiC twins observed by Zhang et al.[17] were synthesized with Cu and 50 vol% $Ti_3AlC_2$, meaning that more Al atoms (>2.8 mol%) remained in the $TiC_x$ grains and more TiC nanotwins remained during the fourth step. The solid solubility of Ti in Cu is much lower than that of Al in Cu (about 18% at room temperature[33]), being only approximately 0.4% at room temperature[34] and 6–9% at 882 °C.[35,36] No Cu–Ti or Cu–Al–Ti intermetallics formed; therefore, nearly all the directly contacted Ti atoms remained in the unstable microtwinned structure. The third step [Fig. 6(d)] barely proceeded, preventing the twins from merging into a large size and leading to the formation of more transition zones. In the present study, because nearly all the Al atoms de-intercalated and the Ti atoms in direct contact diffused out of the $TiC_x$ grains to react with Ni, both the third and fourth steps proceeded successfully and nearly completely. Thus, in contrast to the results of Zhang et al.,[17] TiC twinning platelets of large size without high density were observed in the present study.

However, the above proposed mechanism cannot elucidate the structure of the twin boundary in greater detail. An important aspect that remains to be clarified is the distribution of Al within the CTB. Yu and co-workers[11] assumed that the Al was distributed periodically in the CTB. However, it is not clear at present whether the distribution of Al impurities at the CTB is similar to that reported by Nie et al., where the solute atoms segregated periodically at the CTB to reduce the elastic strain energy.[37] A more detailed characterization of the twin boundary on the atomic scale is required to determine this, which is outside the scope of the present paper.

Yu et al. have attempted to produce TiC twins with Ti, C, and Al elemental powders as starting materials.[11] However, only SFs but no TiC twins were observed. Therefore, it can be concluded that the energy barrier for the transformation from TiC to the twinned structure is relatively high. Because of the high energy barrier and intrinsic instability, few successful syntheses of TiC twins have been reported. The present study provides an opportunity to use nanolaminated $Ti_nA_mX_{n-m}$ (A is an A group element, X is C and/or N, and $n \geq 2m$) compounds[38] as precursors to obtain TiC twinning platelets to strengthen and toughen TiC or TiC-containing ceramics.

## V. CONCLUSIONS

TiC twinning platelets were formed by the reaction between $Ti_3AlC_2$ and Ni. Apart from perfect twins, defective twins with a certain degree of deviation from the perfect orientation were observed. In addition, SFs were identified in the TiC twins. The twin boundaries are of three types, CTB, ITB1, and ITB2. The Al atoms that remained in the TiC twins segregate at the twin boundaries. A mechanism for the formation and stabilization of TiC twinning platelets is proposed. This mechanism can be divided into four steps: (1) de-intercalation of Al atoms from the $Ti_3C_2$ skeleton; (2) relaxation of the $Ti_3C_2$ microtwinned structure; (3) de-intercalation of Ti atoms; and (4) de-twinning and merging of the asymmetric TiC microtwins.

## ACKNOWLEDGMENT

This work is supported by the Chinese Academy of Sciences.

## REFERENCES

1. S.D. Luo, Q. Li, J. Tian, C. Wang, M. Yan, G.B. Schaffer, and M. Qian: Self-assembled, aligned TiC nanoplatelet-reinforced titanium composites with outstanding compressive properties. *Scripta Mater.* **69**(1), 29 (2013).
2. M. Hsu, M. Meyers, and A. Berkowitz: Synthesis of nanocrystalline titanium carbide by spark erosion. *Scripta Metall. Mater.* **32**(6), 805 (1995).
3. D. Gu, G. Meng, C. Li, W. Meiners, and R. Poprawe: Selective laser melting of TiC/Ti bulk nanocomposites: Influence of nanoscale reinforcement. *Scripta Mater.* **67**(2), 185 (2012).
4. M. Sherif El-Eskandarany: Structure and properties of nanocrystalline TiC full-density bulk alloy consolidated from mechanically reacted powders. *J. Alloys Comp.* **305**(1), 225 (2000).
5. A. Sen, T. Kar, and S.K. Pradhan: One step quickest mechanosynthesis of nanocrystalline $Ti_{0.9}Si_{0.1}C$ and its microstructure characterization. *J. Alloys Comp.* **557**(0), 47 (2013).
6. K. Lu: The future of metals. *Science* **328**(5976), 319 (2010).
7. Y. Tian, B. Xu, D. Yu, Y. Ma, Y. Wang, Y. Jiang, W. Hu, C. Tang, Y. Gao, K. Luo, Z. Zhao, L.M. Wang, B. Wen, J. He, and Z. Liu: Ultrahard nanotwinned cubic boron nitride. *Nature* **493**(7432), 385 (2013).
8. I. Gutierrez-Urrutia and D. Raabe: Multistage strain hardening through dislocation substructure and twinning in a high strength and ductile weight-reduced Fe–Mn–Al–C steel. *Acta Mater.* **60**(16), 5791 (2012).



https://doi.org/10.1557/jmr.2014.80 Published online by Cambridge University Press

9. J. Zhang and Y.C. Zhou: Microstructure, mechanical, and electrical properties of Cu–$Ti_3AlC_2$ and in situ Cu–$TiC_x$ composites. *J. Mater. Res.* **23**(4), 924 (2008).
10. R. Yu, Q. Zhan, L.L. He, Y.C. Zhou, and H.Q. Ye: Si-induced twinning of TiC and formation of $Ti_3SiC_2$ platelets. *Acta Mater.* **50**(16), 4127 (2002).
11. R. Yu, L.L. He, and H.Q. Ye: Effects of Si and Al on twin boundary energy of TiC. *Acta Mater.* **51**(9), 2477 (2003).
12. W.T. Hu, S.C. Liu, B. Wen, J.Y. Xiang, F.S. Wen, B. Xu, J.L. He, D.L. Yu, Y.J. Tian, and Z.Y. Liu: {111}-specific twinning structures in nonstoichiometric $ZrC_{0.6}$ with ordered carbon vacancies. *J. Appl. Crystallogr.* **46**(1), 43 (2013).
13. H. Zhang, X.H. Wang, Z.J. Li, M.Y. Liu, and Y.C. Zhou: A novel $Ni_2AlTi$-containing composite with excellent wear resistance and anomalous flexural strength. *Mater. Sci. Eng., A* **597**(0), 70 (2014).
14. B.J. Kooi, M. Kabel, A.B. Kloosterman, and J.T.M. De Hosson: Reaction layers around SiC particles in Ti: an electron microscopy study. *Acta Mater.* **47**(10), 3105 (1999).
15. F.R. Chien, S.R. Nutt, and D. Cummings: Defect structures in single crystal TiC. *Philos. Mag. A* **68**(2), 325 (1993).
16. J. Venables: Stacking faults in TiC. *Phys. Status Solidi B* **15**(1), 413 (1966).
17. J. Zhang, J.Y. Wang, and Y.C. Zhou: Structure stability of $Ti_3AlC_2$ in Cu and microstructure evolution of Cu–$Ti_3AlC_2$ composites. *Acta Mater.* **55**(13), 4381 (2007).
18. Y.C. Zhou, Z.M. Sun, and B.H. Yu: Microstructure of $Ti_3SiC_2$ prepared by the in-situ hot pressing/solid–liquid reaction process. *Z. Metallkd.* **91**(11), 937 (2000).
19. Y.C. Zhou and Z.M. Sun: Crystallographic relations between $Ti_3SiC_2$ and TiC. *Mater. Res. Innovat.* **3**(5), 286 (2000).
20. X.H. Wang and Y.C. Zhou: Solid–liquid reaction synthesis of layered machinable $Ti_3AlC_2$ ceramic. *J. Mater. Chem.* **12**(3), 455 (2002).
21. Z.J. Lin, M.J. Zhuo, Y.C. Zhou, M.S. Li, and J.Y. Wang: Microstructural characterization of layered ternary $Ti_2AlC$. *Acta Mater.* **54**(4), 1009 (2006).
22. U. Wolf, F. Ernst, T. Muschik, M.W. Finnis, and H.F. Fischmeister: The influence of grain boundary inclination on the structure and energy of $\sum = 3$ grain boundaries in copper. *Philos. Mag. A* **66**(6), 991 (1992).
23. L. Liu, J. Wang, S.K. Gong, and S.X. Mao: High resolution transmission electron microscope observation of zero-strain deformation twinning mechanisms in Ag. *Phys. Rev. Lett.* **106**(17), 175504 (2011).
24. J. Wang, O. Anderoglu, J.P. Hirth, A. Misra, and X. Zhang: Dislocation structures of sigma 3{112} twin boundaries in face centered cubic metals. *Appl. Phys. Lett.* **95**(2), 021908 (2009).
25. J. Bezares, S. Jiao, Y. Liu, D. Bufford, L. Lu, X. Zhang, Y. Kulkarni, and R.J. Asaro: Indentation of nanotwinned fcc metals: implications for nanotwin stability. *Acta Mater.* **60**(11), 4623 (2012).
26. V.Y. Markiv, V.V. Burnashova, and V.R. Riabov: A study of the Ti–Fe–Al, Ti–Ni–Al, and Ti–Cu–Al systems. *Metallofizika* **46**(46), 103 (1973).
27. K. Zeng, R. Schmid-Fetzer, B. Huneau, P. Rogl, and J. Bauer: The ternary system Al–Ni–Ti part II: thermodynamic assessment and experimental investigation of polythermal phase equilibria. *Intermetallics* **7**(12), 1347 (1999).
28. J.P. Buban, K. Matsunaga, J. Chen, N. Shibata, W.Y. Ching, T. Yamamoto, and Y. Ikuhara: Grain boundary strengthening in alumina by rare earth impurities. *Science* **311**(5758), 212 (2006).
29. Z. Wang, M. Saito, K.P. McKenna, L. Gu, S. Tsukimoto, A.L. Shluger, and Y. Ikuhara: Atom-resolved imaging of ordered defect superstructures at individual grain boundaries. *Nature* **479**(7373), 380 (2011).
30. Y.M. Chiang, A.F. Henriksen, W.D. Kingery, and D. Finello: Characterization of grain-boundary segregation in MgO. *J. Am. Ceram. Soc.* **64**(7), 385 (1981).
31. R.J. Kerans, K.S. Mazdiyasni, R. Ruh, and H.A. Lipsitt: Solubility of metals in substoichiometric $TiC_{1-x}$. *J. Am. Ceram. Soc.* **67**(1), 34 (1984).
32. N. Shibata, S.J. Pennycook, T.R. Gosnell, G.S. Painter, W.A. Shelton, and P.F. Becher: Observation of rare-earth segregation in silicon nitride ceramics at subnanometre dimensions. *Nature* **428**(6984), 730 (2004).
33. A. Varschavsky and E. Donoso: The kinetics of disperse order development in α-CuAl alloys. *Metall. Trans. A* **14**(4), 875 (1983).
34. F.R. Hensel and E.I. Larsen: Age-hardening copper–titanium alloys. *Trans. Am. Inst. Min. Metall. Eng.* **99**, 55 (1932).
35. M.V. Itkin and O.A. Shmatko: On the temperature-concentration bound of cellular decomposition in Cu–Ti system. *Phys. Met.* **4**(4), 806 (1982).
36. H. Okamoto: Cu–Ti (copper–titanium). *J. Phase Equilib.* **23**(6), 549 (2002).
37. J.F. Nie, Y.M. Zhu, J.Z. Liu, and X.Y. Fang: Periodic segregation of solute atoms in fully coherent twin boundaries. *Science* **340**(6135), 957 (2013).
38. H. Zhang, X.H. Wang, Y.H. Ma, L.C. Sun, L.Y. Zheng, and Y.C. Zhou: Crystal structure determination of nanolaminated $Ti_5Al_2C_3$ by combined techniques of XRPD, TEM and ab initio calculations. *J. Adv. Ceram.* **1**(4), 268 (2012).


https://doi.org/10.1557/jmr.2014.80 Published online by Cambridge University Press